Spatial Attentive Single-Image Deraining with a High Quality Real Rain Dataset

Tianyu Wang[1,2*] Xin Yang[1,2*] Ke Xu[1,2] Shaozhe Chen[1] Qiang Zhang[1] Rynson W.H. Lau[2†]
[1]Dalian University of Technology [2]City University of Hong Kong

Overview. In this supplemental, we first visualize the generated attention maps to demonstrate the effectiveness of the proposed SPANet in detecting the rain regions in Section 1. We then provide additional comparisons between our SPANet and state-of-the-art single-image derainers on real rain images on the proposed benchmark and from the Internet in Sections 2 and 3, respectively. In Section 4, we provide results of the state-of-the-art video deraining methods, mode filter and our proposed background generation method on synthetic rain videos.

1. Visualization of the Attention Maps

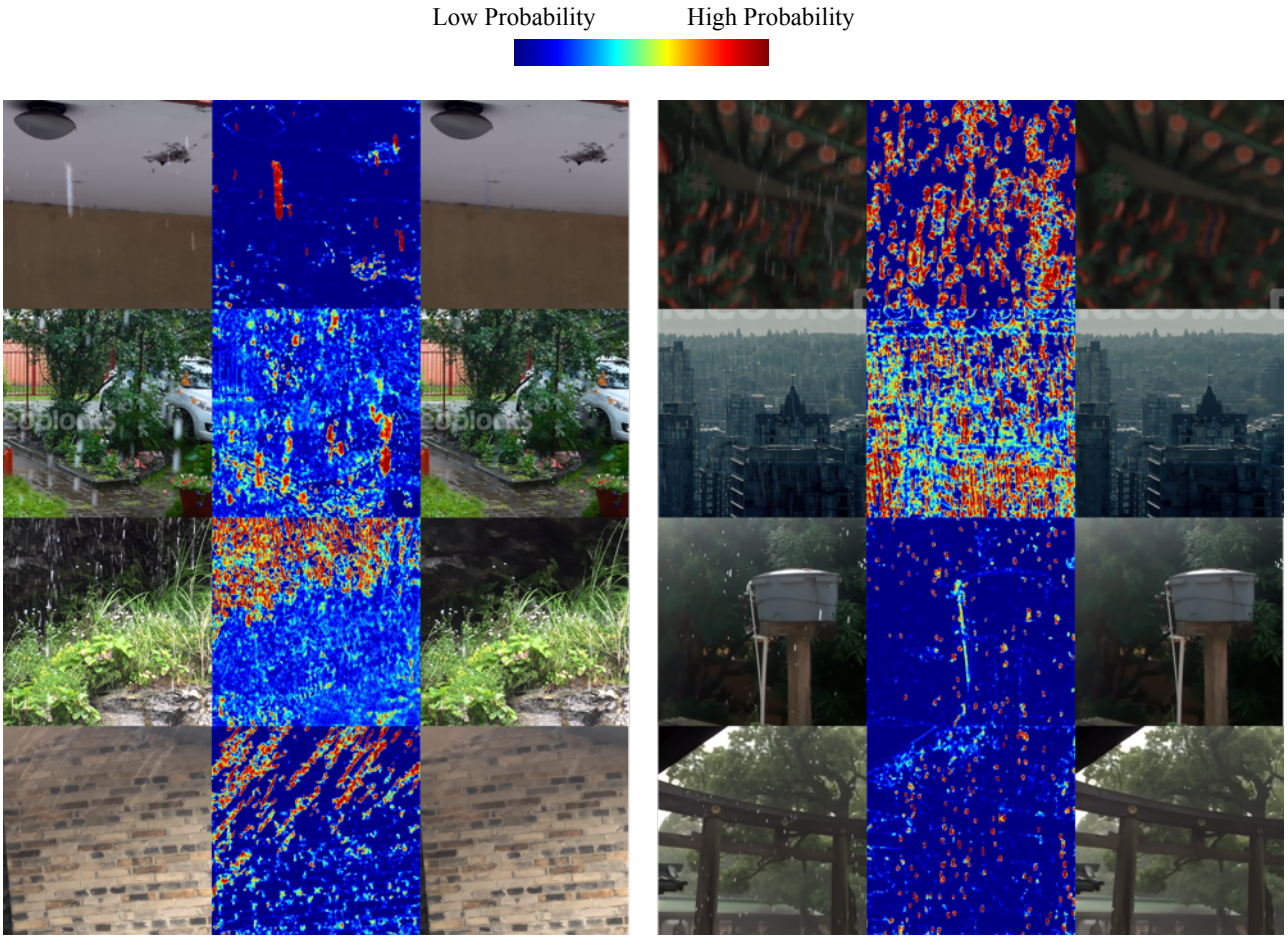

(a) Rain Image (b) Our Attention Map (c) SPANet Result (d) Rain Image (e) Our Attention Map (f) SPANet Result

Figure 1. Visualization of the attention maps generated by our SPANet.

* Joint first authors. † Rynson Lau is the corresponding author, and he led this project.

2. Comparison on Real Rain Images from the Proposed Benchmark

(a) Rain Image 29.17 / 0.9130 (b) DSC [8] 29.51 / 0.9108 (c) LP [7] 30.95 / 0.9286

(d) SILS [3] 30.44 / 0.9186 (e) Clearing [1] 28.64 / 0.9029 (f) DDN [2] 30.01 / 0.9207

(g) JORDER [10] 28.54 / 0.9054 (h) DID-MDN [11] 21.27 / 0.7701 (i) RESCAN [6] 30.31 / 0.9201

(j) DDN [2] 38.36 / 0.9668 (k) JORDER [10] 33.13 / 0.9445 (l) DID-MDN [11] 34.57 / 0.9548

(m) RESCAN [6] 34.82 / 0.9605 **(n) Our SPANet 39.69 / 0.9874** (o) Clean Image ∞ / 1

Figure 2. Comparison on real rain images. Methods in red were trained on the proposed dataset. PSNR/SSIM results are included for reference.

(a) Rain Image 34.51 / 0.9343

(b) DSC [8] 35.5 / 0.9366

(c) LP [7] 39.09 / 0.9755

(d) SILS [3] 39.46 / 0.9753

(e) Clearing [1] 35.82 / 0.9632

(f) DDN [2] 39.59 / 0.9747

(g) JORDER [10] 37.07 / 0.9689

(h) DID-MDN [11] 16.87 / 0.8267

(i) RESCAN [6] 38.74 / 0.9734

(j) DDN [2] 41.83 / 0.9770

(k) JORDER [10] 43.26 / 0.9835

(l) DID-MDN [11] 19.11 / 0.8844

(m) RESCAN [6] 35.14 / 0.9740

(n) Our SPANet 48.72 / 0.9956

(o) Clean Image ∞ / 1

Figure 3. Comparison on real rain images. Methods in red were trained on the proposed dataset. PSNR/SSIM results are included for reference.

(a) Rain Image 32.48 / 0.9380 (b) DSC [8] 33.23 / 0.9374 (c) LP [7] 33.44 / 0.9396

(d) SILS [3] 33.52 / 0.9359 (e) Clearing [1] 31.38 / 0.9221 (f) DDN [2] 34.36 / 0.9455

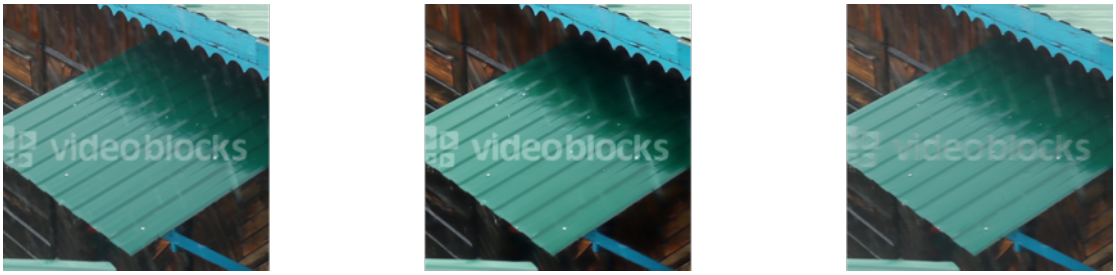

(g) JORDER [10] 33.41 / 0.9265 (h) DID-MDN [11] 24.87 / 0.8372 (i) RESCAN [6] 30.75 / 0.9138

(j) DDN [2] 35.67 / 0.9541 (k) JORDER [10] 36.42 / 0.9597 (l) DID-MDN [11] 28.63 / 0.9218

(m) RESCAN [6] 34.97 / 0.9536 **(n) Our SPANet 37.78 / 0.9743** (o) Clean Image ∞ / 1

Figure 4. Comparison on real rain images. Methods in red were trained on the proposed dataset. PSNR/SSIM results are included for reference.

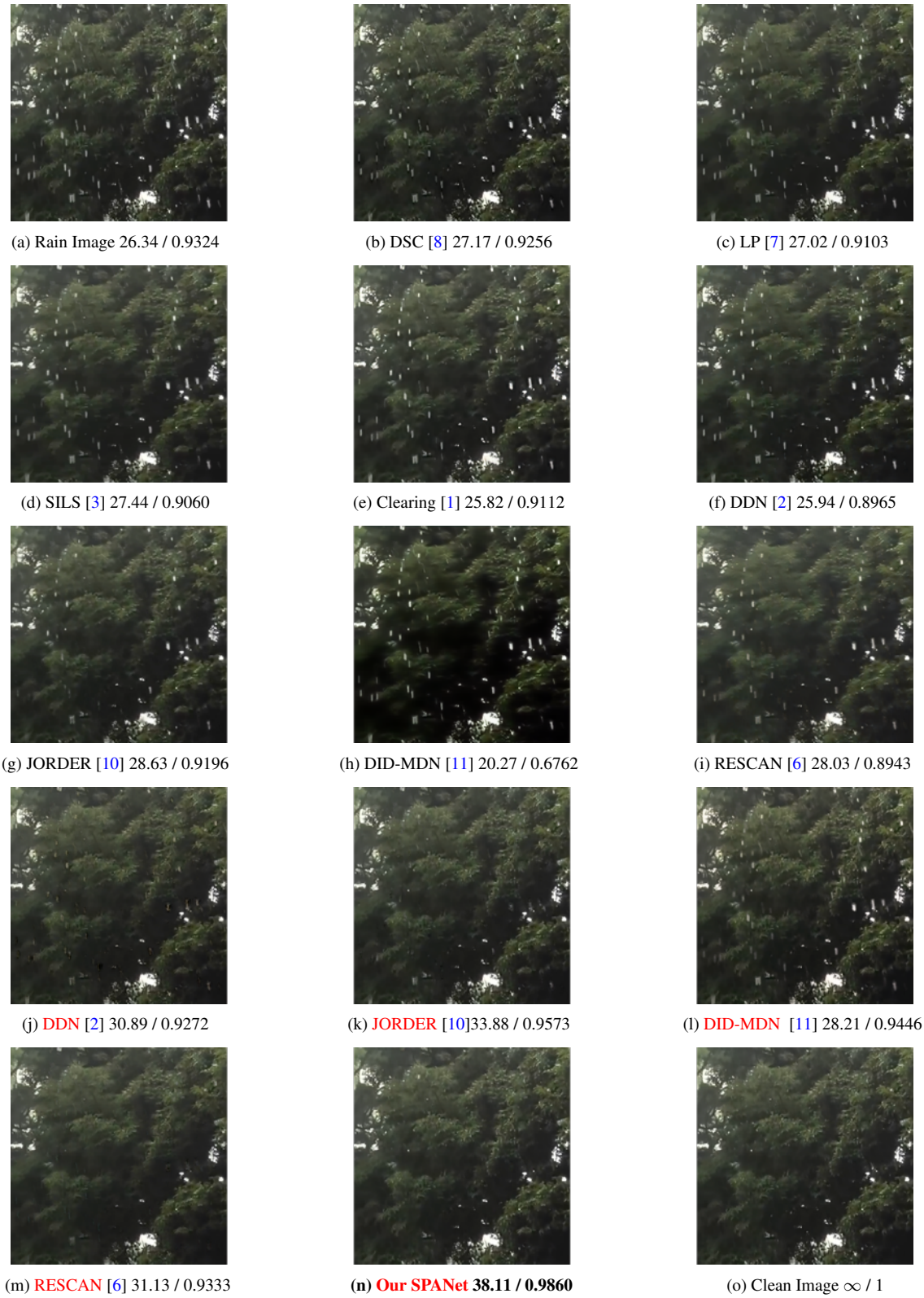

(a) Rain Image 26.34 / 0.9324 (b) DSC [8] 27.17 / 0.9256 (c) LP [7] 27.02 / 0.9103

(d) SILS [3] 27.44 / 0.9060 (e) Clearing [1] 25.82 / 0.9112 (f) DDN [2] 25.94 / 0.8965

(g) JORDER [10] 28.63 / 0.9196 (h) DID-MDN [11] 20.27 / 0.6762 (i) RESCAN [6] 28.03 / 0.8943

(j) DDN [2] 30.89 / 0.9272 (k) JORDER [10]33.88 / 0.9573 (l) DID-MDN [11] 28.21 / 0.9446

(m) RESCAN [6] 31.13 / 0.9333 **(n) Our SPANet 38.11 / 0.9860** (o) Clean Image ∞ / 1

Figure 5. Comparison on real rain images. Methods in red were trained on the proposed dataset. PSNR/SSIM results are included for reference.

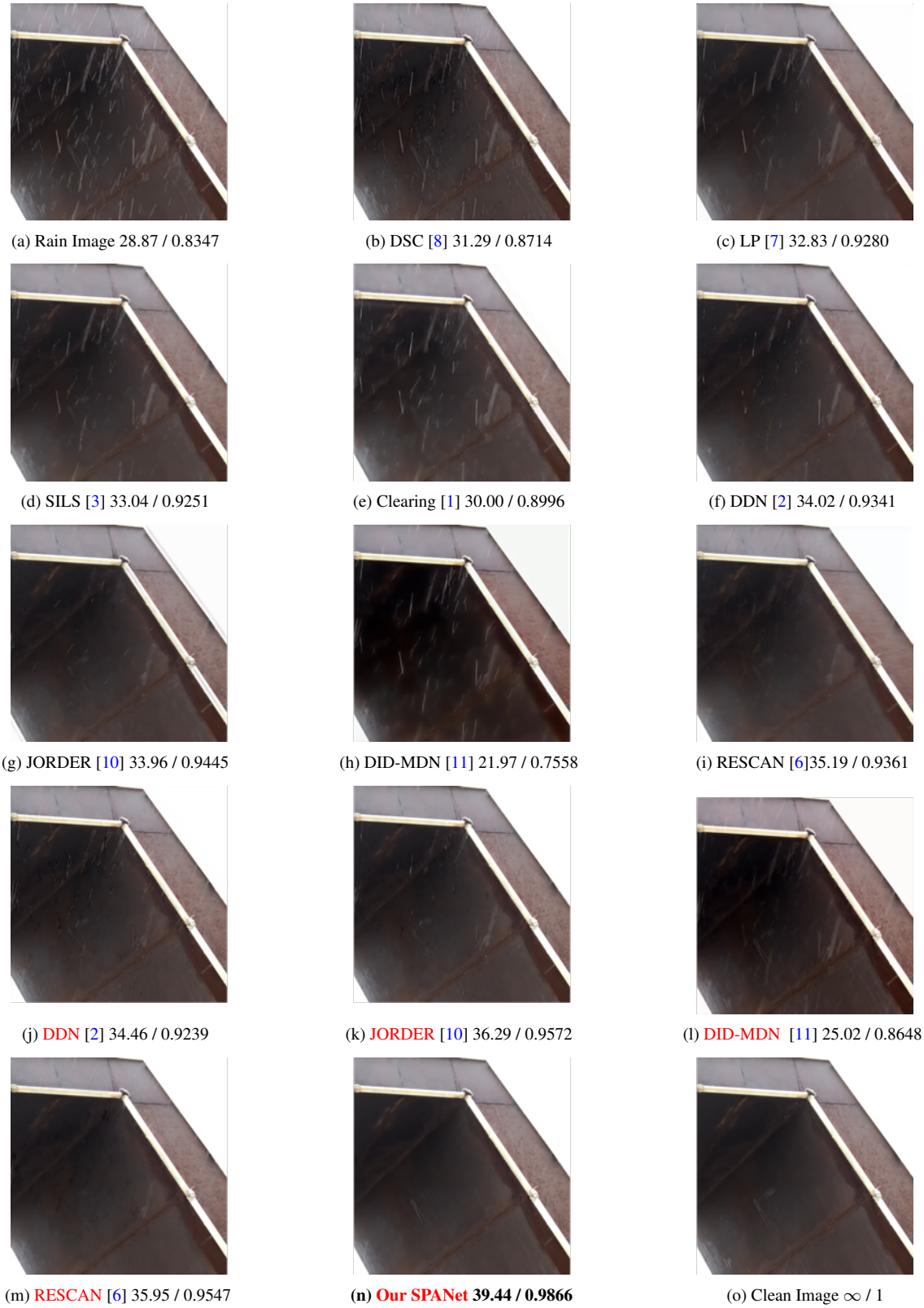

(a) Rain Image 28.87 / 0.8347 (b) DSC [8] 31.29 / 0.8714 (c) LP [7] 32.83 / 0.9280

(d) SILS [3] 33.04 / 0.9251 (e) Clearing [1] 30.00 / 0.8996 (f) DDN [2] 34.02 / 0.9341

(g) JORDER [10] 33.96 / 0.9445 (h) DID-MDN [11] 21.97 / 0.7558 (i) RESCAN [6]35.19 / 0.9361

(j) DDN [2] 34.46 / 0.9239 (k) JORDER [10] 36.29 / 0.9572 (l) DID-MDN [11] 25.02 / 0.8648

(m) RESCAN [6] 35.95 / 0.9547 **(n) Our SPANet 39.44 / 0.9866** (o) Clean Image ∞ / 1

Figure 6. Comparison on real rain images. Methods in red were trained on the proposed dataset. PSNR/SSIM results are included for reference.

(a) Rain Image 31.03 / 0.8398

(b) DSC [8] 33.31 / 0.8636

(c) LP [7] 34.42 / 0.9186

(d) SILS [3] 35.02 / 0.9265

(e) Clearing [1] 32.36 / 0.9069

(f) DDN [2] 34.65 / 0.9135

(g) JORDER [10] 35.29 / 0.9319

(h) DID-MDN [11] 27.60 / 0.8378

(i) RESCAN [6] 30.24 / 0.8919

(j) DDN [2] 34.48 / 0.9050

(k) JORDER [10]35.86 / 0.9384

(l) DID-MDN [11] 31.56 / 0.9128

(m) RESCAN [6] 35.73 / 0.9304

(n) Our SPANet 38.63 / 0.9749

(o) Clean Image ∞ / 1

Figure 7. Comparison on real rain images. Methods in red were trained on the proposed dataset. PSNR/SSIM results are included for reference.

(a) Rain Image 28.21 / 0.9228 (b) DSC [8] 28.67 / 0.9228 (c) LP [7] 29.83 / 0.9384

(d) SILS [3] 30.09 / 0.9447 (e) Clearing [1] 28.44 / 0.9274 (f) DDN [2] 29.57 / 0.9459

(g) JORDER [10] 32.67 / 0.9565 (h) DID-MDN [11] 18.89 / 0.7420 (i) RESCAN [6]32.52 / 0.9531

(j) DDN [2] 35.24 / 0.9574 (k) JORDER [10] 35.42 / 0.9672 (l) DID-MDN [11] 22.47 / 0.8680

(m) RESCAN [6] 35.45 / 0.9674 **(n) Our SPANet 43.83 / 0.9926** (o) Clean Image ∞ / 1

Figure 8. Comparison on real rain images. Methods in red were trained on the proposed dataset. PSNR/SSIM results are included for reference.

(a) Rain Image 31.90 / 0.9427

(b) DSC [8] 33.42 / 0.9465

(c) LP [7] 33.54 / 0.9467

(d) SILS [3] 33.14 / 0.9541

(e) Clearing [1] 31.03 / 0.9409

(f) DDN [2] 33.97 / 0.9551

(g) JORDER [10] 31.30 / 0.9416

(h) DID-MDN [11] 25.07 / 0.9365

(i) RESCAN [6] 31.20 / 0.9461

(j) DDN [2] 35.70 / 0.9636

(k) JORDER [10]35.42 / 0.9641

(l) DID-MDN [11] 32.58 / 0.9559

(m) RESCAN [6] 34.39 / 0.9627

(n) Our SPANet 38.28 / 0.9803

(o) Clean Image ∞ / 1

Figure 9. Comparison on real rain images. Methods in red were trained on the proposed dataset. PSNR/SSIM results are included for reference.

3. Comparison on Real Rain Images Obtained from the Internet

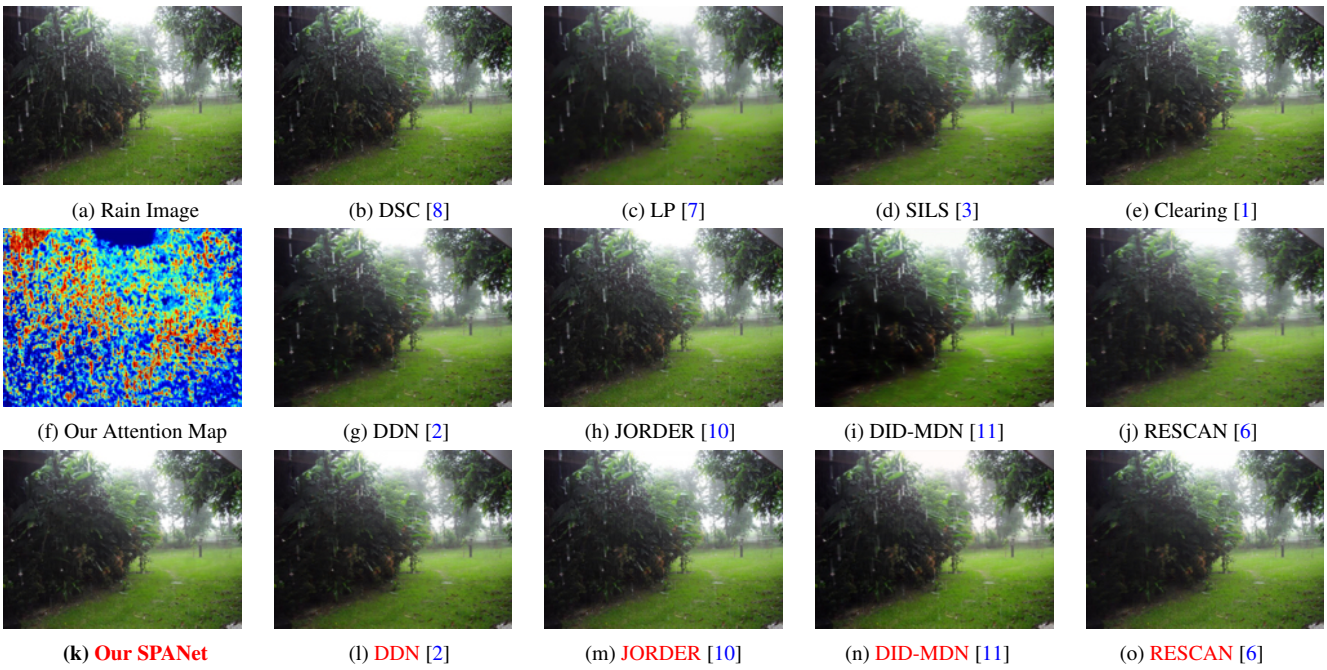

(a) Rain Image (b) DSC [8] (c) LP [7] (d) SILS [3] (e) Clearing [1]

(f) Our Attention Map (g) DDN [2] (h) JORDER [10] (i) DID-MDN [11] (j) RESCAN [6]

(k) Our SPANet (l) DDN [2] (m) JORDER [10] (n) DID-MDN [11] (o) RESCAN [6]

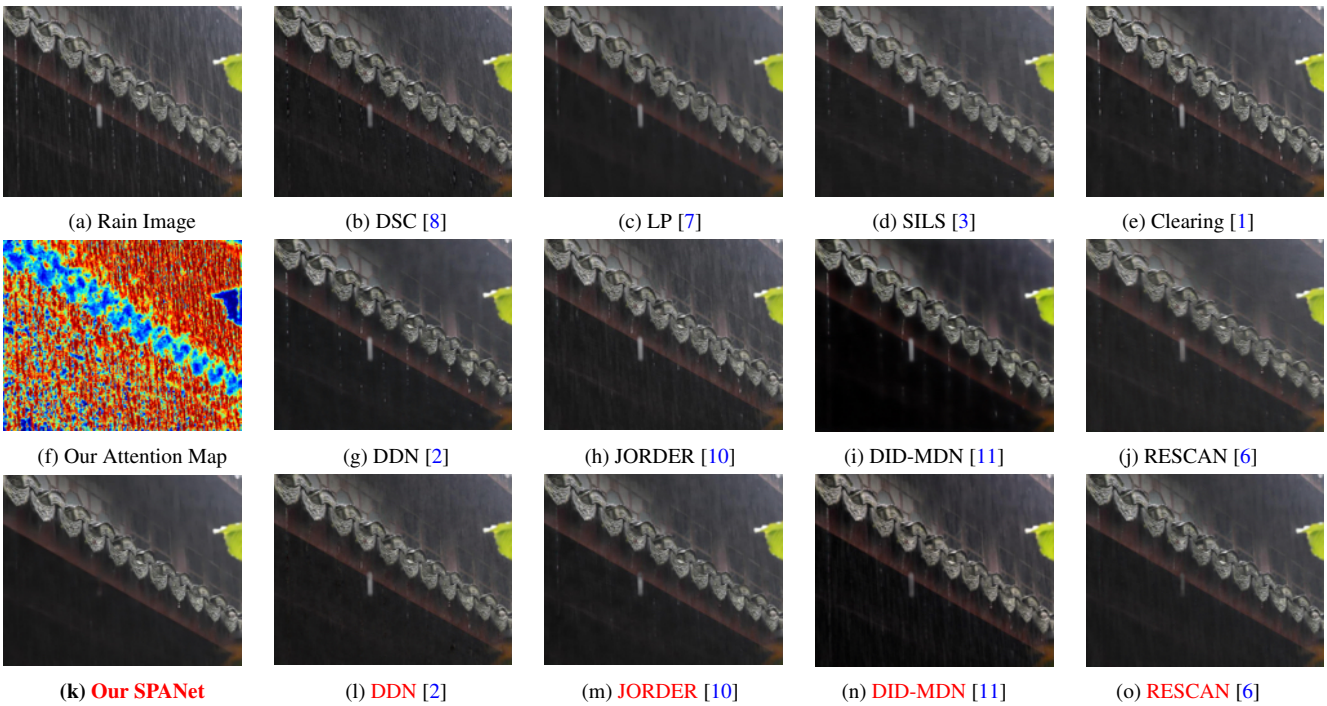

(a) Rain Image (b) DSC [8] (c) LP [7] (d) SILS [3] (e) Clearing [1]

(f) Our Attention Map (g) DDN [2] (h) JORDER [10] (i) DID-MDN [11] (j) RESCAN [6]

(k) Our SPANet (l) DDN [2] (m) JORDER [10] (n) DID-MDN [11] (o) RESCAN [6]

Figure 10. Comparison on real rain images obtained from the Internet. Methods in red were trained on the proposed dataset.

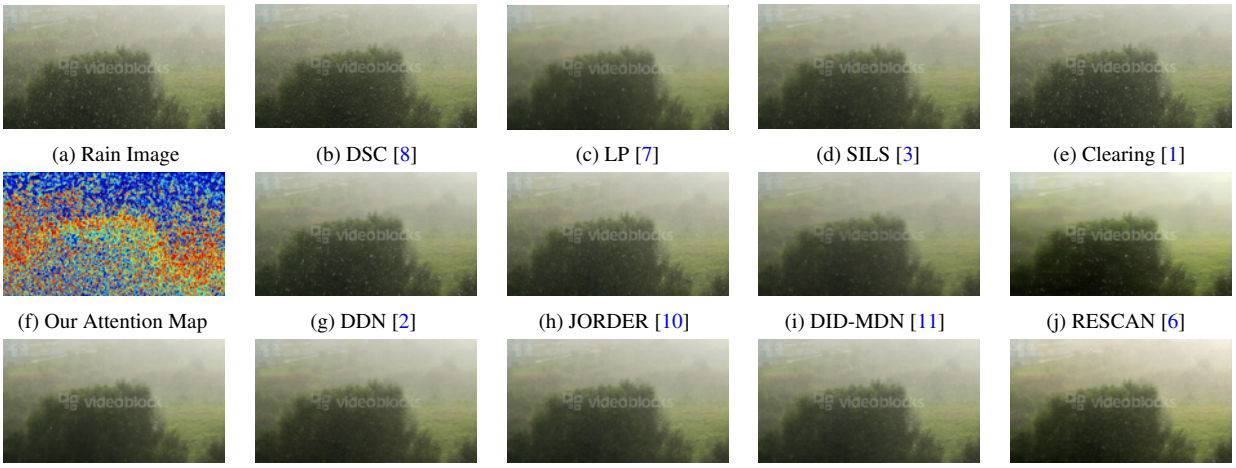

(a) Rain Image (b) DSC [8] (c) LP [7] (d) SILS [3] (e) Clearing [1]

(f) Our Attention Map (g) DDN [2] (h) JORDER [10] (i) DID-MDN [11] (j) RESCAN [6]

(k) Our SPANet (l) DDN [2] (m) JORDER [10] (n) DID-MDN [11] (o) RESCAN [6]

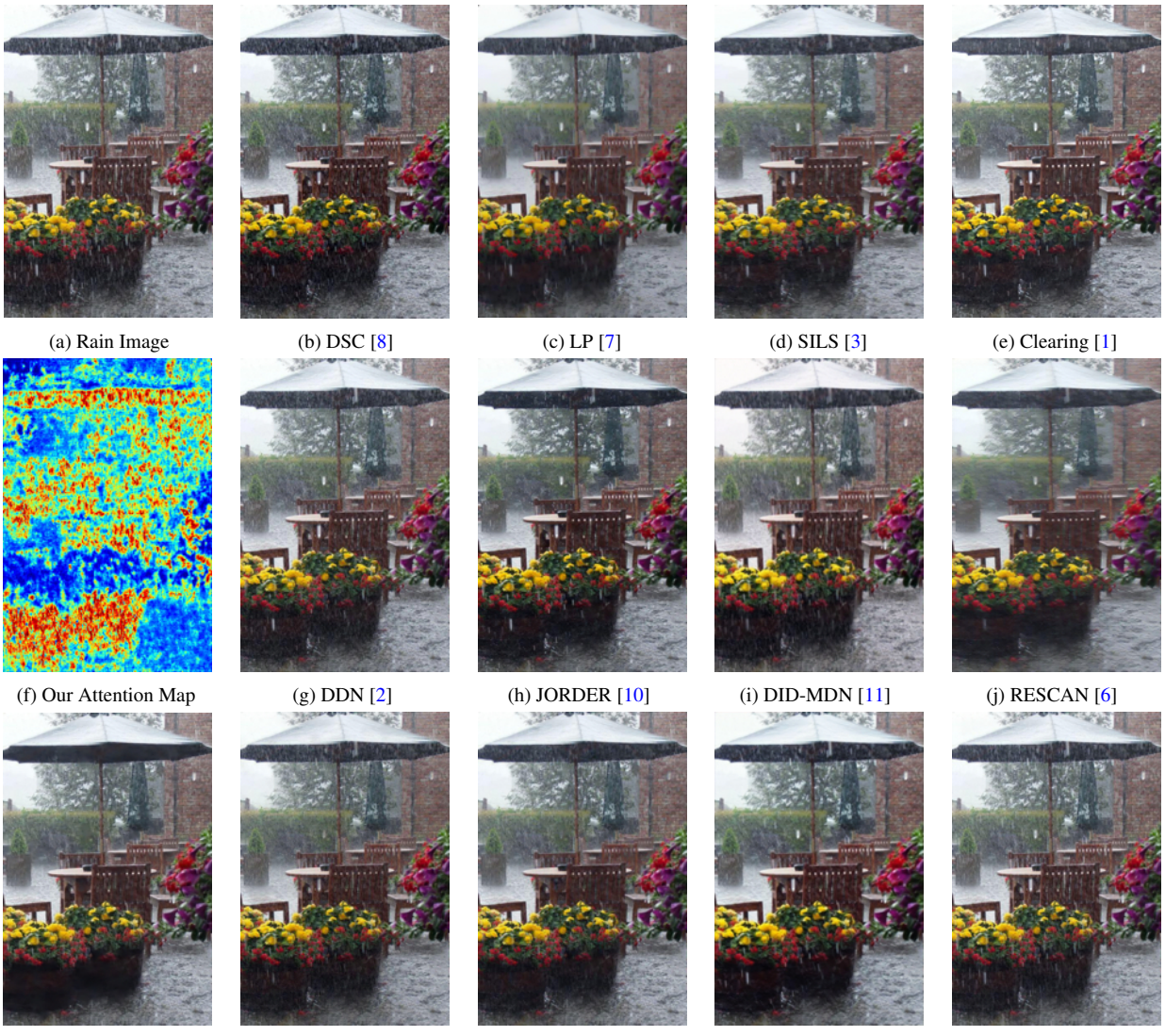

(a) Rain Image (b) DSC [8] (c) LP [7] (d) SILS [3] (e) Clearing [1]

(f) Our Attention Map (g) DDN [2] (h) JORDER [10] (i) DID-MDN [11] (j) RESCAN [6]

(k) Our SPANet (l) DDN [2] (m) JORDER [10] (n) DID-MDN [11] (o) RESCAN [6]

Figure 11. Comparison on real rain images obtained from the Internet. Methods in red were trained on the proposed dataset.

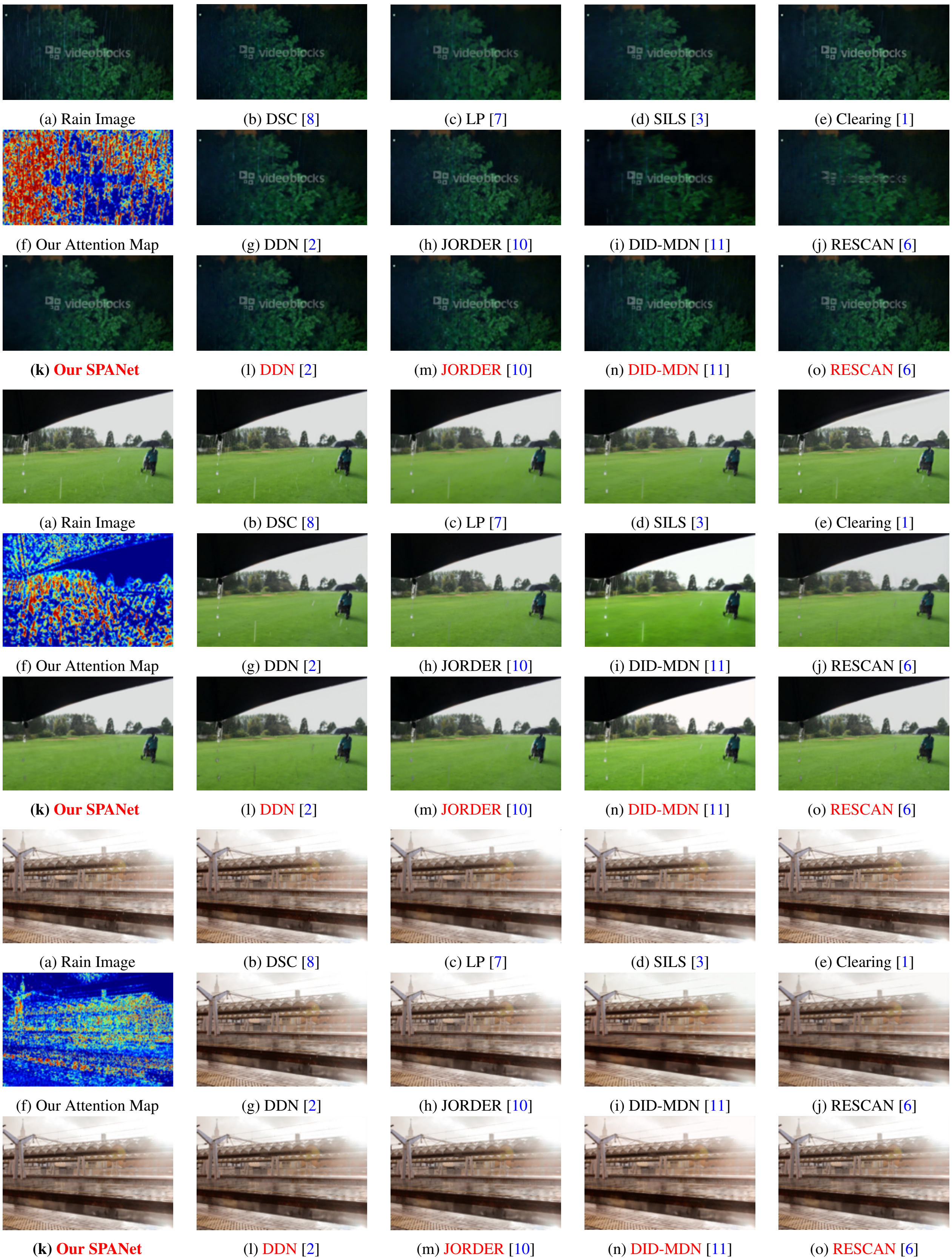

(a) Rain Image (b) DSC [8] (c) LP [7] (d) SILS [3] (e) Clearing [1]

(f) Our Attention Map (g) DDN [2] (h) JORDER [10] (i) DID-MDN [11] (j) RESCAN [6]

(k) Our SPANet (l) DDN [2] (m) JORDER [10] (n) DID-MDN [11] (o) RESCAN [6]

(a) Rain Image (b) DSC [8] (c) LP [7] (d) SILS [3] (e) Clearing [1]

(f) Our Attention Map (g) DDN [2] (h) JORDER [10] (i) DID-MDN [11] (j) RESCAN [6]

(k) Our SPANet (l) DDN [2] (m) JORDER [10] (n) DID-MDN [11] (o) RESCAN [6]

(a) Rain Image (b) DSC [8] (c) LP [7] (d) SILS [3] (e) Clearing [1]

(f) Our Attention Map (g) DDN [2] (h) JORDER [10] (i) DID-MDN [11] (j) RESCAN [6]

(k) Our SPANet (l) DDN [2] (m) JORDER [10] (n) DID-MDN [11] (o) RESCAN [6]

Figure 12. Comparison on real rain images obtained from the Internet. Methods in red were trained on the proposed dataset.

4. Comparison on Synthetic Rain Videos for Dataset Generation Methods

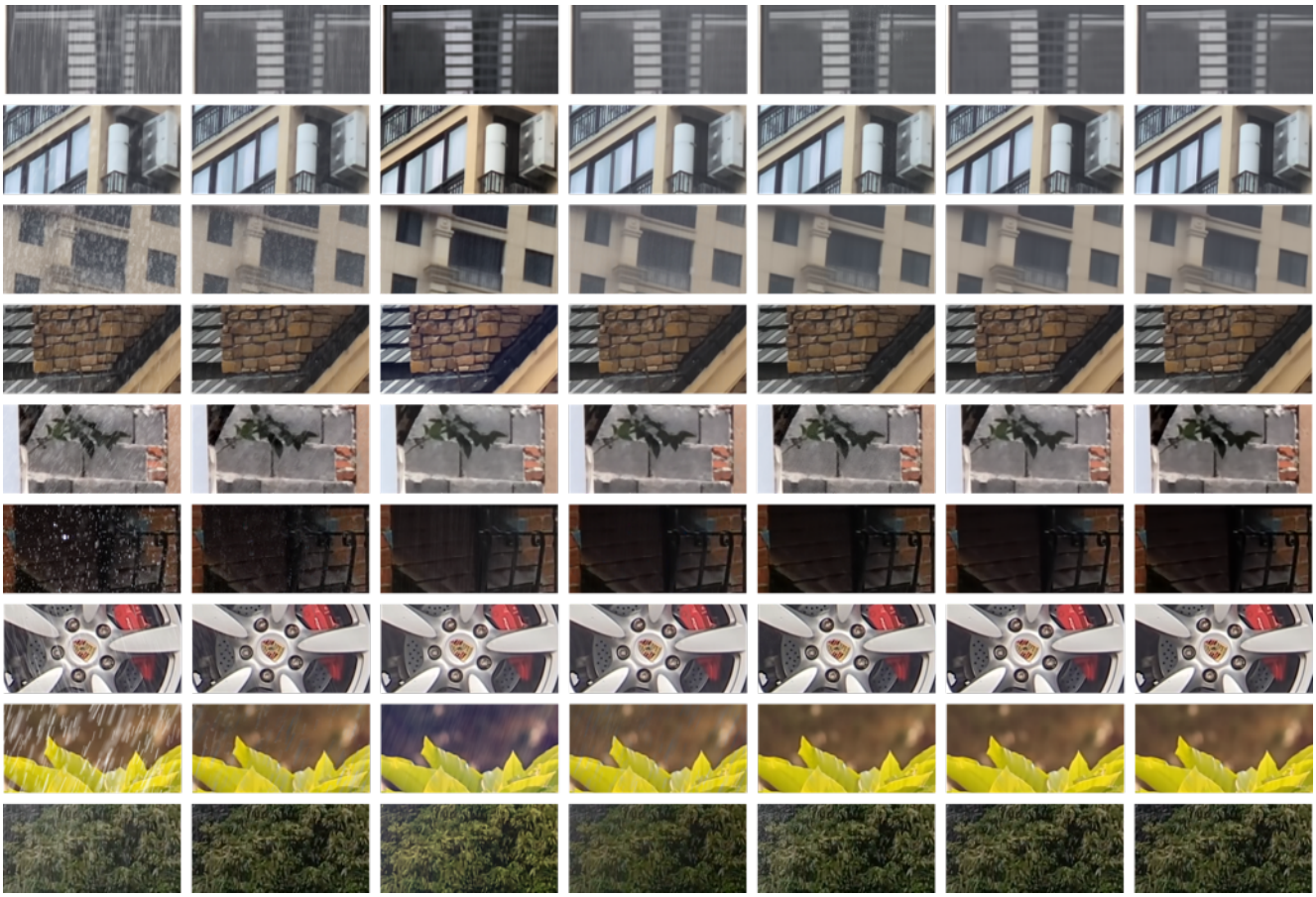

(a) Input (b) Jiang [4] (b) Wei [9] (d) Li [5] (e) Mode (f) **Ours** (g) Ground Truth

Figure 13. Comparison on synthetic rain videos of 100 frames. Our dataset generation method can get clearer background than other state-of-the-art video derain methods and mode filter.

References

[1] Xueyang Fu, Jiabin Huang, Xinghao Ding, Yinghao Liao, and John Paisley. Clearing the skies: A deep network architecture for single-image rain streaks removal. *IEEE TIP*, 2017. 2, 3, 4, 5, 6, 7, 8, 9, 10, 11, 12

[2] Xueyang Fu, Jiabin Huang, Delu Zeng, Yue Huang, Xinghao Ding, and John Paisley. Removing rain from single images via a deep detail network. In *CVPR*, 2017. 2, 3, 4, 5, 6, 7, 8, 9, 10, 11, 12

[3] Shuhang Gu, Deyu Meng, Wangmeng Zuo, and Lei Zhang. Joint convolutional analysis and synthesis sparse representation for single image layer separation. In *ICCV*, 2017. 2, 3, 4, 5, 6, 7, 8, 9, 10, 11, 12

[4] Tai-Xiang Jiang, Ting-Zhu Huang, Xi-Le Zhao, Liang-Jian Deng, and Yao Wang. A novel tensor-based video rain streaks removal approach via utilizing discriminatively intrinsic priors. In *CVPR*, 2017. 13

[5] Minghan Li, Qi Xie, Qian Zhao, Wei Wei, Shuhang Gu, Jing Tao, and Deyu Meng. Video rain streak removal by multiscale convolutional sparse coding. In *CVPR*, 2018. 13

[6] Xia Li, Jianlong Wu, Zhouchen Lin, Hong Liu, and Hongbin Zha. Recurrent squeeze-and-excitation context aggregation net for single image deraining. In *ECCV*, 2018. 2, 3, 4, 5, 6, 7, 8, 9, 10, 11, 12

[7] Yu Li, Robby T Tan, Xiaojie Guo, Jiangbo Lu, and Michael Brown. Rain streak removal using layer priors. In *CVPR*, 2016. 2, 3, 4, 5, 6, 7, 8, 9, 10, 11, 12

[8] Yu Luo, Yong Xu, and Hui Ji. Removing rain from a single image via discriminative sparse coding. In *ICCV*, 2015. 2, 3, 4, 5, 6, 7, 8, 9, 10, 11, 12

[9] Wei Wei, Lixuan Yi, Qi Xie, Qian Zhao, Deyu Meng, and Zongben Xu. Should we encode rain streaks in video as deterministic or stochastic? In *ICCV*, 2017. 13

[10] Wenhan Yang, Robby T Tan, Jiashi Feng, Jiaying Liu, Zongming Guo, and Shuicheng Yan. Deep joint rain detection and removal from a single image. In *CVPR*, 2017. 2, 3, 4, 5, 6, 7, 8, 9, 10, 11, 12

[11] He Zhang and Vishal M. Patel. Density-aware single image de-raining using a multi-stream dense network. In *CVPR*, 2018. 2, 3, 4, 5, 6, 7, 8, 9, 10, 11, 12